PNAS
www.pnas.org

Supplementary Information for

An image-computable model on how endogenous and exogenous attention differentially alter visual perception

Michael Jigo[1*], David J. Heeger[1,2] & Marisa Carrasco[1,2]

[1] Center for Neural Science and [2] Department of Psychology
New York University, New York, NY 10003

[*] **Corresponding author information**:
Michael Jigo
Center for Neural Science
New York University
6 Washington Place, Room 974
New York, NY 1003
michael.jigo@nyu.edu

This PDF file includes:

Supplementary Text
Figures S1 to S7
Tables S1 to S6

Supplementary Information Text

Extended Materials and Methods

S1 Optimization strategy

S1.1 Central performance drop

We fit the model jointly to performance on the neutral condition of all 10 texture segmentation experiments (103 data points). Peripheral and central cueing conditions (for exogenous and endogenous attentional conditions, respectively) were excluded to isolate the CPD. 15 free parameters fit all 103 data points (**Table S2**). Ten separate free parameters independently controlled the minimum contrast gain at the fovea (g_σ; equation 15) for each of the 10 experiments. Sensitivity to contrast and SF varies for stimuli placed at isoeccentric locations around the visual field; it is higher at the horizontal meridian and decreases gradually towards the vertical meridian (1-4). Whereas 5 out of 6 exogenous attention experiments used targets placed on the horizontal meridian, 3 out of 4 endogenous attention experiments used targets presented along the intercardinal meridians (**Table S5**). Because SF selectivity depends on stimulus polar angle, two parameters separately determined the highest preferred SF (t_T; equation 3)—one shared among exogenous attention experiments and the other shared among endogenous attention experiments. Alternatively, we could have fit separate parameters for horizontal, vertical and intercardinal meridians. However, this approach would have added a third free parameter, reducing the parsimony of the model. The configuration we used yielded reasonably good fits.

The remaining three parameters were shared among all experiments. Each controlled the bandwidth (b_T; equation 2) of the tuning function T, the gradual shift toward lower SFs with eccentricity (m_T; equation 3) and the increase in contrast gain across eccentricity (m_σ; equation 15).

S1.2 Attentional modulation

To generate the effects of attention, the model was fit separately to exogenous and endogenous attention experiments. We jointly fit the model to neutral and valid conditions of each experiment.

Exogenous attention. All six exogenous attention experiments were fit jointly (146 data points) with 14 free parameters (**Table S3**). Minimum contrast gain at the fovea (g_σ; equation 15) was determined independently for each of six experiments, yielding six free parameters. The remaining eight parameters were shared among all experiments. Four determined the stimulus drive: its

bandwidth (b_T; equation 2), the highest preferred SF at the fovea (t_T; equation 3), the shift to lower SFs with eccentricity (m_T; equation 3) and the slope of contrast gain across eccentricity (m_σ; equation 15). The remaining four controlled the narrow SF attentional gain profile, specifically its bandwidth (b_N; equation 7), center SF (λ_N; equation 8), the shift to lower SFs with eccentricity (m_N; equation 8), and its amplitude (γ_N; equation 10).

Endogenous attention. All four endogenous attention experiments were fit jointly (60 data points) with 12 free parameters (**Table S4**). Minimum contrast gain at the fovea (g_σ; equation 15) was determined independently for each experiment, which yielded four free parameters. The remaining eight parameters were shared among experiments, as described above for exogenous attention.

S2 Model comparisons

We compared models using AIC (5) and BIC (6). The difference in AIC/BIC values between model variants indexed model performance. '-θ', '-f', '-x,y', '-all' and '-sum' models were compared to the full model. Additionally, narrow and broad SF gain profiles as well as the spatial extent model were compared.

S3 Stimulus generation

Target-present and target-absent textures were re-created to match the stimulus parameters used in each psychophysical study (**Table S5**). For all stimuli, each pixel subtended 0.03125° (i.e., 32 pixels/°), roughly matching the spatial resolution of a 1280 × 960 monitor display placed 57 cm away from the observer.

The full texture stimulus used in each experiment typically spanned the entire display. We generated 5°-wide square cutouts of the texture stimulus, centered on the target location. Because the model implemented visual sensitivity that varied with eccentricity, but was uniform at isoeccentric locations, all targets were assumed to be presented along the horizontal eccentricity for simplicity (as in equation 6).

Each texture array was composed of lines oriented 135°. The target comprised a patch of lines that were oriented 45°. One study was an exception (7) because the texture array comprised vertical lines (0°) and the target patch contained lines tilted ±8° (**Figure 3D**). In this study, observers'

performed an orientation discrimination task by reporting the orientation of the target presented on each trial. To simulate orientation discrimination performance, the target-present and target-absent stimuli always contained a patch but their orientation differed.

To avoid edge artifacts, texture stimuli were windowed by the sum of three cosine window functions (as in equation 8) centered on the target that produced a uniform plateau covering the central 3.75 deg and fell off with cosine edges. Pixel intensities in each stimulus were constrained between 0 and 1.

Textures used to fit the model were generated without spatial or orientation jittering. In additional simulations, the stimuli of two representative experiments were jittered. The stimuli for Experiment 1 in (8) were spatially jittered (0.3 deg jitter), and the stimuli in Experiment 4 in (9), were jittered spatially (0.34 deg jitter) and in orientation (55° bandwidth). Jitter parameters were compatible with those specified in each study.

S4 Resampling procedures

We obtained confidence intervals on the parameter estimates, model predictions and AIC/BIC values by bootstrapping the data and refitting the model 100 times per configuration (see **SI Appendix, section S1**) and for each model variant (see **Methods, Model alternatives**). Bootstrap samples were generated by drawing and fitting random samples from Gaussian distributions centered on group-average performance at a given eccentricity, with the SEM for each study defining the distribution's width.

To generate bootstrap samples for simulations with jittered texture stimuli, the model was first fit to the data for each experiment using a non-jittered texture. Then, the model parameters were fixed and jittered stimuli were input to the model. This procedure allowed us to assess how a fixed model behaved with variable texture inputs. One hundred unique jittered stimuli were presented to the model.

S5 Cross-validation procedure

To characterize how the operating range of exogenous and endogenous attention varied with eccentricity, relative to baseline tuning preferences (**Figure S2-S3**), we fit polynomials to empirical measurements made by (10). Leave-one-subject-out cross-validation determined the best-fitting polynomial order. Specifically, the ratio, in octaves, between the peak SF of the neutral contrast sensitivity function and the preferred SF of attentional modulation were computed for individual observers. Eccentricities were aggregated between each of the two experiments conducted. The ratio for one observer was set aside, and the remaining were averaged. Zero to second-order polynomials were fit to the group-average ratio across eccentricities. The sum of squared error to the left-out data point indexed cross-validation error. This process was iterated until each observation was left-out once, resulting in 19 total iterations. The best-fitting polynomial order was defined as one that produced the lowest median cross-validation error across all iterations.

S6 Model generalizability to basic visual tasks

We applied the same observer model to behavioral data from tasks mediated by acuity (11) and contrast sensitivity (10). The model was configured identically to what is described in **Methods, Model** and the same model parameters were fit to behavioral data using BADS (12). To simulate the Neutral condition, attentional gain was not included in the model. Narrow SF and broad SF gain profiles were used to simulate all exogenous and endogenous attentional effects, respectively.

S6.1 Acuity

The modeling strategy for the acuity task is outlined in **Figure S6**. Landolt squares were inputted to the model with stimulus parameters that matched those described in (11). The squares were 1°-wide Landolt squares with a line thickness of 0.05°. Images were padded with 0.5° of empty space on each side to avoid edge artifacts. Model responses were computed for Landolt squares with a small gap (<1°) on the top or bottom. The Eucledian norm of the difference between responses indexed localization performance in the task. The model was evaluated at the eccentricity tested in the experiment (9.375°) and at 10 linearly spaced gap sizes (0-30 arcmin). We characterized the full psychometric function by interpolating between gap sizes. Interpolation was used to reduce computational load; similar psychometric functions were generated when the model was evaluated at finer intervals. The available signal for discrimination was scaled so that the maximum d′ equaled 2 and gap thresholds were quantified as the gap size needed to attain d′=1. For each attention type, 10 free parameters were fit to 14 gap thresholds (7 observers x 2 cueing conditions (Neutral, Valid)).

S6.2 Contrast sensitivity

The modeling strategy for the contrast sensitivity task is outlined in **Figure S7**. Tilted gratings (±45°) were inputted to the model with stimulus parameters that matched those described in (10). Gratings were windowed by a cosine function with a FWHM of 2°, had one of 6 SFs (0.5, 1, 2, 4 and 8 cpd) and were simulated at each of the four eccentricities tested (0°, 3°, 6° and 12°). We omitted the highest SF tested in (10) because it fell outside the range of SF subbands (0.5-8 cpd) used to simulate texture segmentation performance. Grating images were padded with 0.5° of empty space on each side to avoid edge artifacts.

To simulate the signal available to an observer in the orientation discrimination task, we computed the Eucledian norm of the difference between orthogonal gratings. This procedure was repeated for each grating SF and eccentricity. Model population responses were evaluated at 7 log-spaced levels of contrast that were interpolated to characterize the full contrast response function (**Figure S7C**). Similar contrast response functions were produced when the model was evaluated at finer contrast steps. We scaled the available signal by the magnitude of internal noise to yield stimulus discriminability (see **Methods, Decision mechanism**). Because internal noise varies with SF (13), the available signal was scaled such that the maximum d′ at the fovea equaled 2 for each SF. Contrast thresholds were then determined as the level of contrast required to reach d′=1 and their inverse indexed contrast sensitivity. For each attention type, 10 free parameters were fit to 360 contrast thresholds (9 observers x 2 cueing conditions (neutral, valid) x 4 eccentricities x 5 SFs).

REFERENCES

1. M. Carrasco, C. P. Talgar, E. L. Cameron, Characterizing visual performance fields: Effects of transient covert attention, spatial frequency, eccentricity, task and set size. *Spatial vision* **15**, 61-75 (2001).
2. E. L. Cameron, J. C. Tai, M. Carrasco, Covert attention affects the psychometric function of contrast sensitivity. *Vision Research* **42**, 949-967 (2002).
3. M. M. Himmelberg, J. Winawer, M. Carrasco, Stimulus-dependent contrast sensitivity asymmetries around the visual field. *Journal of vision* **20**, 18-18 (2020).
4. A. Barbot, S. Xue, M. Carrasco, Asymmetries in visual acuity around the visual field. *Journal of Vision* **21**, 2-2 (2021).
5. H. Akaike, A new look at the statistical model identification. *IEEE Trans. Automat. Contr.* **19**, 716-723 (1974).
6. G. Schwarz, Estimating the dimension of a model. *Annals of statistics* **6**, 461-464 (1978).
7. M. Carrasco, F. Loula, Y.-X. Ho, How attention enhances spatial resolution: Evidence from selective adaptation to spatial frequency. *Attention, Perception, & Psychophysics* **68**, 1004-1012 (2006).
8. Y. Yeshurun, M. Carrasco, Attention improves or impairs visual performance by enhancing spatial resolution. *Nature* **396**, 72 (1998).
9. Y. Yeshurun, B. Montagna, M. Carrasco, On the flexibility of sustained attention and its effects on a texture segmentation task. *Vision Research* **48**, 80-95 (2008).
10. M. Jigo, M. Carrasco, Differential impact of exogenous and endogenous attention on the contrast sensitivity function across eccentricity. *Journal of Vision* **20**, 11 (2020).
11. B. Montagna, F. Pestilli, M. Carrasco, Attention trades off spatial acuity. *Vision Research* **49**, 735-745 (2009).
12. L. Acerbi, W. J. Ma, Practical Bayesian optimization for model fitting with Bayesian adaptive direct search. *Advances in neural information processing systems* **30**, 1836-1846 (2017).
13. D. Silvestre, A. Arleo, R. Allard, Internal noise sources limiting contrast sensitivity. *Scientific Reports* **8**, 2596 (2018).
14. C. P. Talgar, M. Carrasco, Vertical meridian asymmetry in spatial resolution: Visual and attentional factors. *Psychonomic Bulletin & Review* **9**, 714-722 (2002).
15. Y. Yeshurun, M. Carrasco, The effects of transient attention on spatial resolution and the size of the attentional cue. *Perception & Psychophysics* **70**, 104-113 (2008).
16. A. Barbot, M. Carrasco, Attention modifies spatial resolution according to task demands. *Psychological science* **28**, 285-296 (2017).

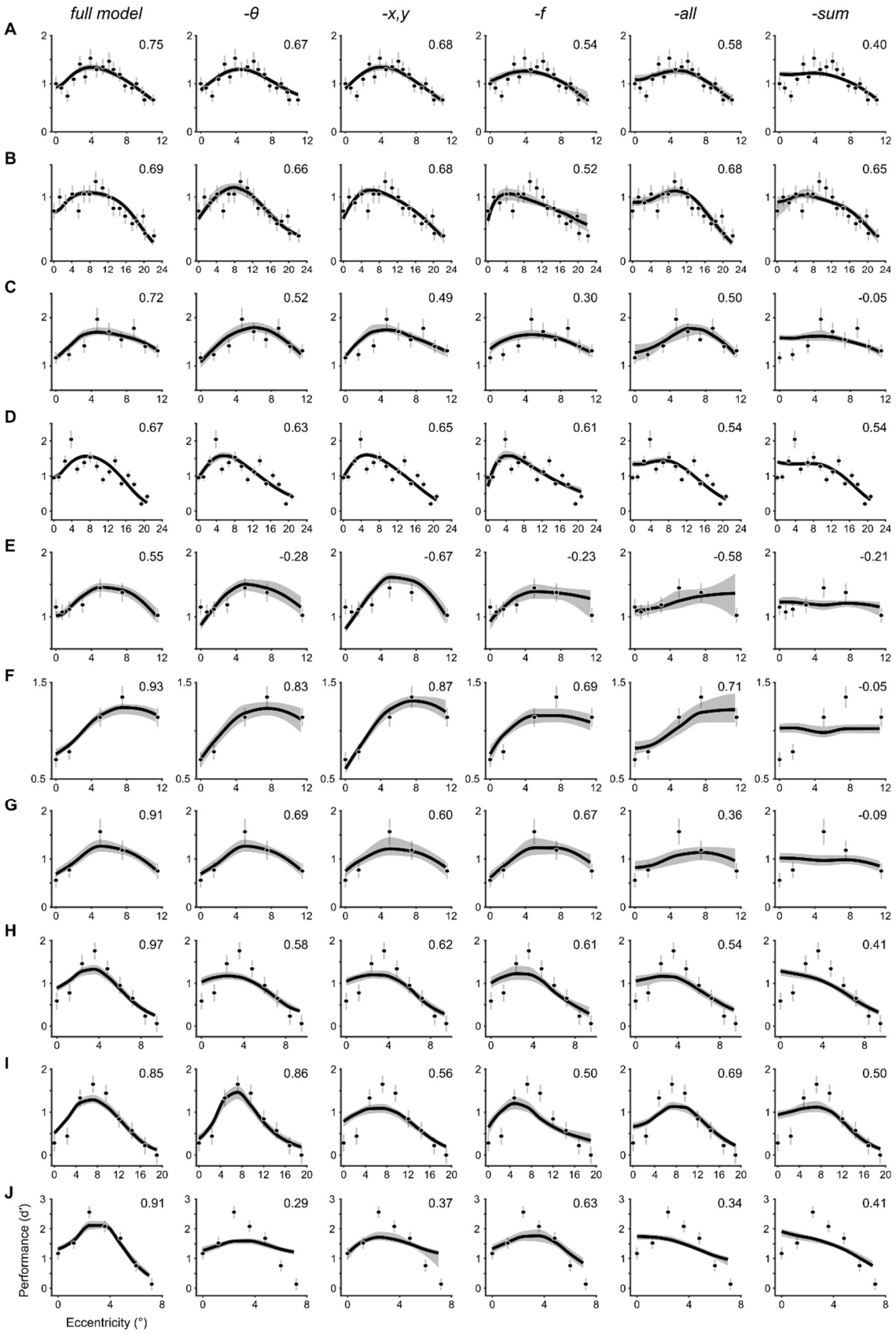
full model
-θ
-x,y
-f
-all
-sum
A
B
C
D
E
F
G
H
I
J
0.75
0.67
0.68
0.54
0.58
0.40
0.69
0.66
0.68
0.52
0.68
0.65
0.72
0.52
0.49
0.30
0.50
-0.05
0.67
0.63
0.65
0.61
0.54
0.54
0.55
-0.28
-0.67
-0.23
-0.58
-0.21
0.93
0.83
0.87
0.69
0.71
-0.05
0.91
0.69
0.60
0.67
0.36
-0.09
0.97
0.58
0.62
0.61
0.54
0.41
0.85
0.86
0.56
0.50
0.69
0.50
0.91
0.29
0.37
0.63
0.34
0.41
Performance (d')
Eccentricity (°)

Figure S1. Model variants fit to the neutral condition of all texture segmentation experiments. Each row depicts the behavioral data from (**A**) Yeshurun & Carrasco, 1998 (8), Experiment 1; (**B**) Yeshurun & Carrasco, 1998 (8), Experiment 2; (**C**) Talgar & Carrasco, 2002 (14); (**D**) Carrasco, Loula & Ho, 2006 (7); (**E**) Yeshurun & Carrasco, 2008 (15); (**F**) Yeshurun, Montagna & Carrasco, 2008 (9), Experiment 2; (**G**) Yeshurun, Montagna & Carrasco, 2008 (9), Experiment 1; (**H**) Yeshurun, Montagna & Carrasco, 2008 (9), Experiment 3; (**I**) Yeshurun, Montagna & Carrasco, 2008 (9), Experiment 4; (**J**) Barbot & Carrasco, 2017 (16). Each column shows the fit of different model variants arranged in order of best-to-worst according to the model comparisons displayed in **Figure 4D**: 'full' denotes the full model, '-θ' lacks cross-orientation suppression, '-x,y' lacks surround suppression, '-f' lacks cross-frequency suppression, '-all' lacks all contextual modulation and '-sum' lacks spatial summation. Dots and error bars denote group-average performance and ±1 SEM. The solid lines depict the median and shaded regions depict 68% confidence intervals of the bootstrapped distribution of model fits. Values in top-right of each panel denote the median R^2 of the bootstrapped distribution of model fits. Negative R^2 values indicate a model fit that captures less variance in the data than a horizontal line passing through the mean d′ across eccentricity.

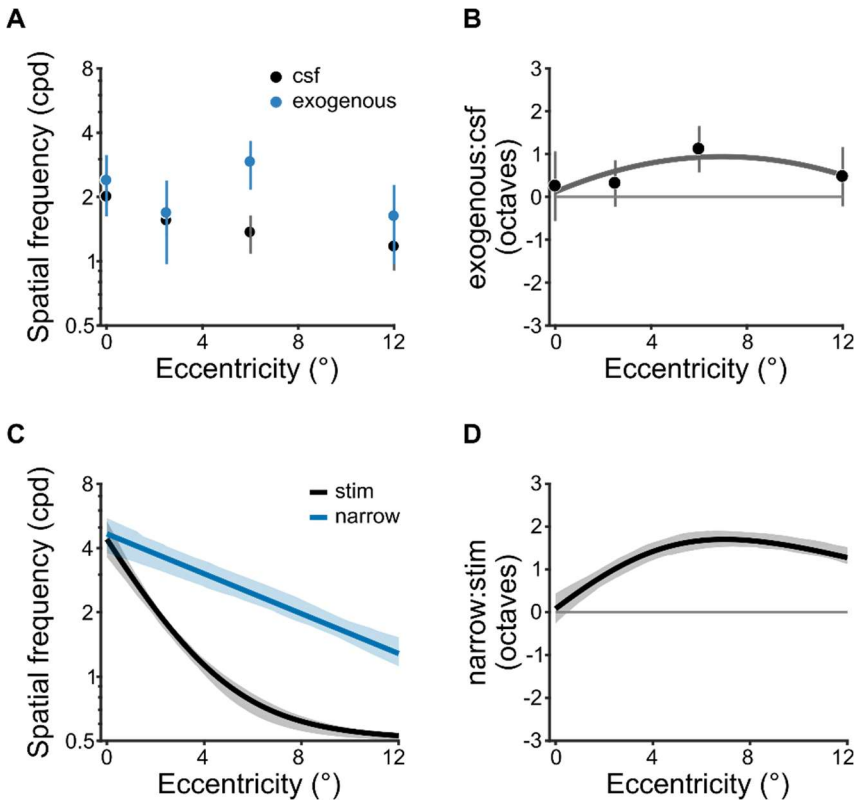

Figure S2. Spatial frequency operating range of exogenous attention.
(**A**) Peak spatial frequency of baseline contrast sensitivity (CSF) and exogenous attentional modulation from Jigo & Carrasco, 2020 (10). Estimates were based on human contrast sensitivity, measured psychophysically with narrowband gratings. (**B**) Ratio (in octaves) of attentional and baseline peak spatial frequency tuning across eccentricity. Positive values denote an attentional preference for spatial frequencies higher than baseline. The solid line depicts the best-fitting second-order polynomial (i.e., parabola). Polynomial order was determined using leave-one-subject-out cross-validation (see **SI Appendix, section S5**). Dots in *A* and *B* depict group-average and error bars depict ±1 SEM. (**C**) Peak spatial frequency of the stimulus drive (stim) and the narrow SF attention gain profile (narrow). Estimates were derived from model fits to texture segmentation performance across all six exogenous attention experiments. (**D**) Ratio of the preferred spatial frequency for the stimulus drive and attentional gain. Solid lines indicate the median and shaded areas denotes 68% confidence interval of bootstrapped distribution in *C* and *D*.

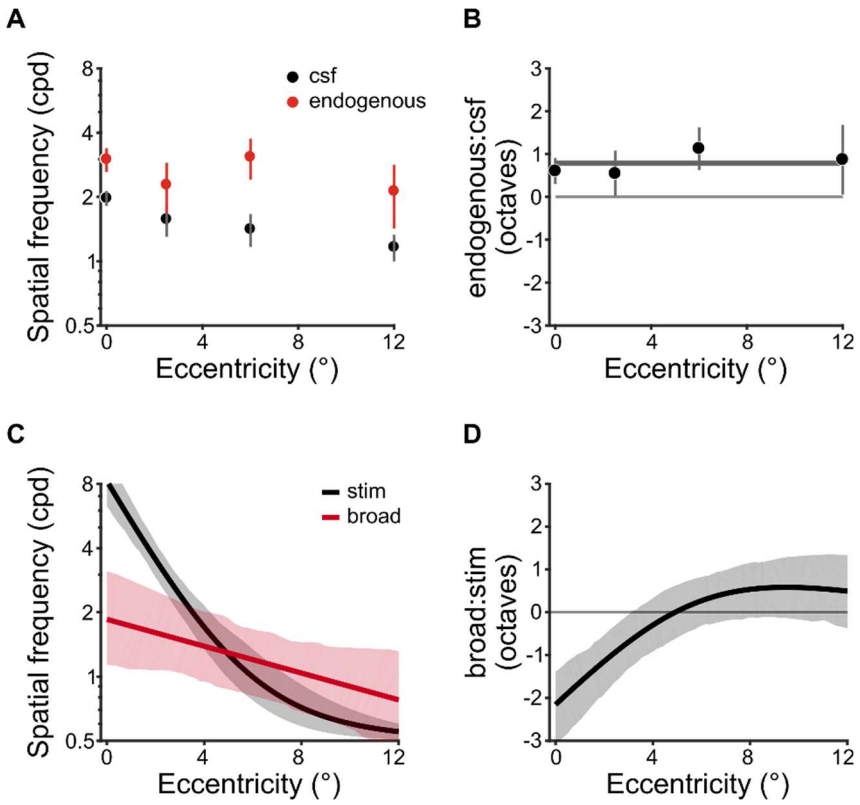

Figure S3. Spatial frequency operating range of endogenous attention.
(**A**) The peak spatial frequency of contrast sensitivity (CSF) and the center frequency of endogenous attentional modulation from Jigo & Carrasco, 2020 (10). Estimates were based on human contrast sensitivity, measured psychophysically with narrowband gratings. (**B**) Ratio (in octaves) of attentional and baseline and spatial frequency preferences across eccentricity. Negative values denote an attentional preference for spatial frequencies lower than baseline. The solid line depicts the best-fitting zero-order polynomial (i.e., constant). Polynomial order was determined using leave-one-subject-out cross-validation (see **SI Appendix, section S5**). Dots in *A* and *B* depict group-average and error bars depict ±1 SEM (**C**) The center spatial frequency of the stimulus drive (stim) and the broad attentional gain profile (broad). Estimates were derived from model fits to texture segmentation performance across all four endogenous attention experiments. (**D**) Ratio of the preferred spatial frequency for the stimulus drive and attentional gain. Solid lines indicate the median and shaded areas denote 68% confidence intervals of the bootstrapped distribution in *C* and *D*.

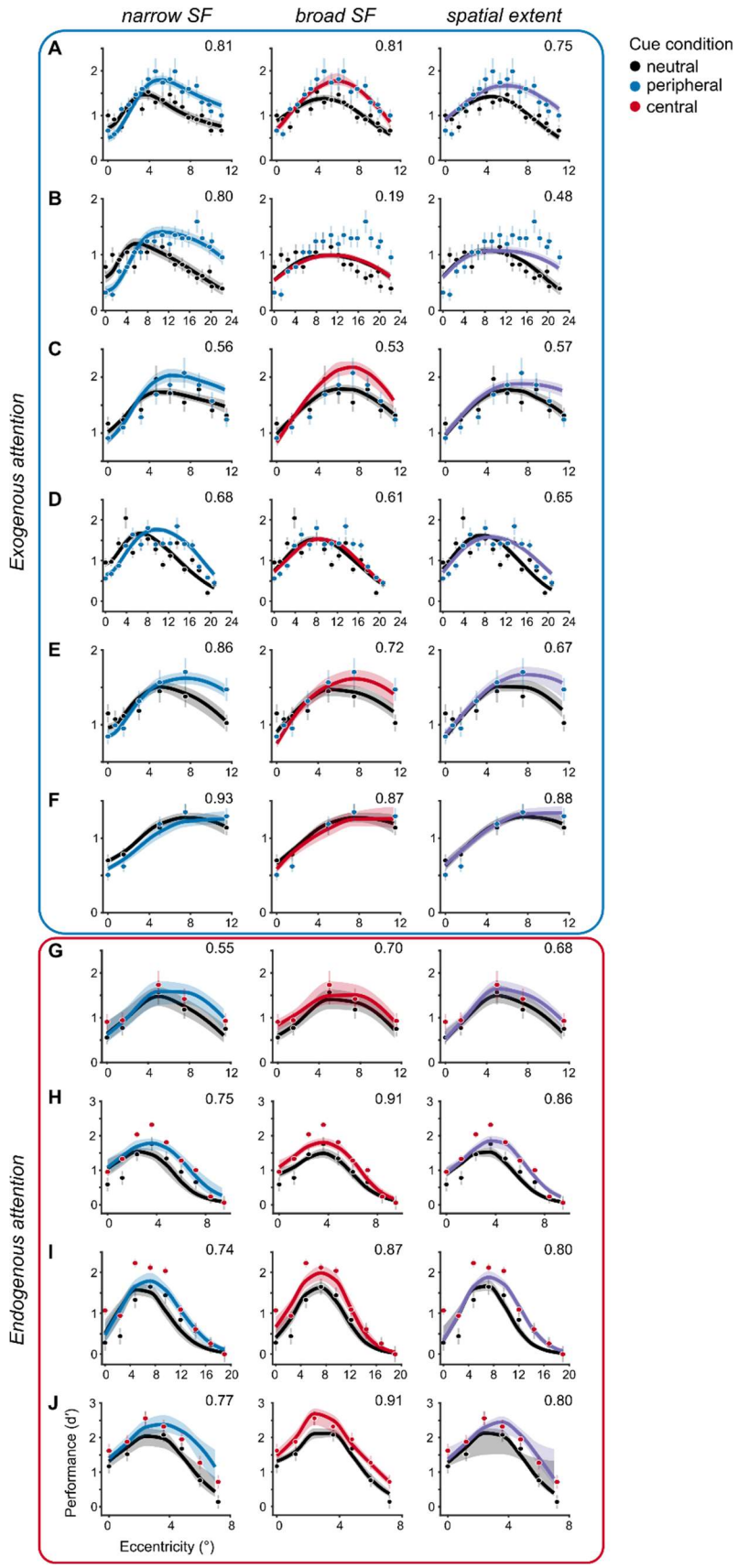
narrow SF
broad SF
spatial extent
Cue condition
neutral
peripheral
central
Exogenous attention
Endogenous attention
A
B
C
D
E
F
G
H
I
J
0.81
0.81
0.75
0.80
0.19
0.48
0.56
0.53
0.57
0.68
0.61
0.65
0.86
0.72
0.67
0.93
0.87
0.88
0.55
0.70
0.68
0.75
0.91
0.86
0.74
0.87
0.80
0.77
0.91
0.80
Performance (d')
Eccentricity (°)

Figure S4. Attention model variants fit to behavioral data of all ten experiments.
Each row depicts a different experiment: (**A**) Yeshurun & Carrasco, 1998 (8), Experiment 1; (**B**) Yeshurun & Carrasco, 1998 (8), Experiment 2; (**C**) Talgar & Carrasco, 2002 (14); (**D**) Carrasco, Loula & Ho, 2006 (7); (**E**) Yeshurun & Carrasco, 2008 (15); (**F**) Yeshurun, Montagna & Carrasco, 2008 (9), Experiment 2; (**G**) Yeshurun, Montagna & Carrasco, 2008 (9), Experiment 1; (**H**) Yeshurun, Montagna & Carrasco, 2008 (9), Experiment 3; (**I**) Yeshurun, Montagna & Carrasco, 2008 (9), Experiment 4; (**J**) Barbot & Carrasco, 2017 (16). Each column depicts a different attentional gain model. The numbers in the top-right of each panel denote the median R^2 of the bootstrapped distribution of model fits.

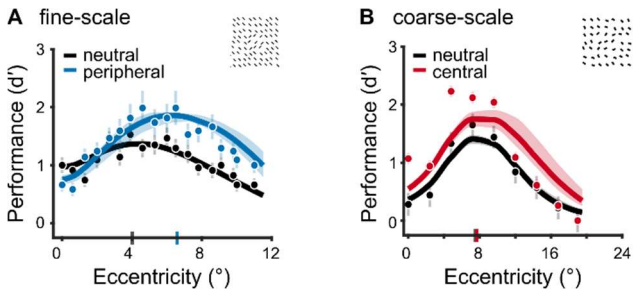

Figure S5. Model fits to jittered texture stimuli.
(**A**) Predicted performance for Experiment 1 in Yeshurun & Carrasco, 1998 (8) using texture stimuli generated with line elements spatially jittered within the stimulus parameters of the experiment (see **SI Appendix, section S3**). An example jittered stimulus is shown in the top-right. Solid lines indicate the median and shaded regions depict 68% confidence intervals of the bootstrap distributions of model predictions. Gray and blue ticks on x-axis indicate peak of performance in the neutral and peripheral cueing condition, respectively. To generate the bootstrap distributions, model parameters were fixed to those that jointly captured all exogenous experiments. Then new jittered texture stimuli were input to the model on each iteration.
(**B**) Predicted performance for Experiment 4 in Yeshurun, Montagna & Carrasco, 2008 (9) using texture stimuli generated with line elements whose orientation and spatial location were randomly jittered within the parameters of the experiment (see **SI Appendix, section S3**). Solid lines indicate the median and shaded regions depict 68% confidence intervals of bootstrap distributions of model predictions. Gray and red ticks on x-axis indicate peak of performance in the neutral and central cueing condition, respectively. To generate the bootstrap distribution, model parameters were fixed to those that jointly captured all endogenous experiments, then new jittered texture stimuli were input to the model on each iteration.

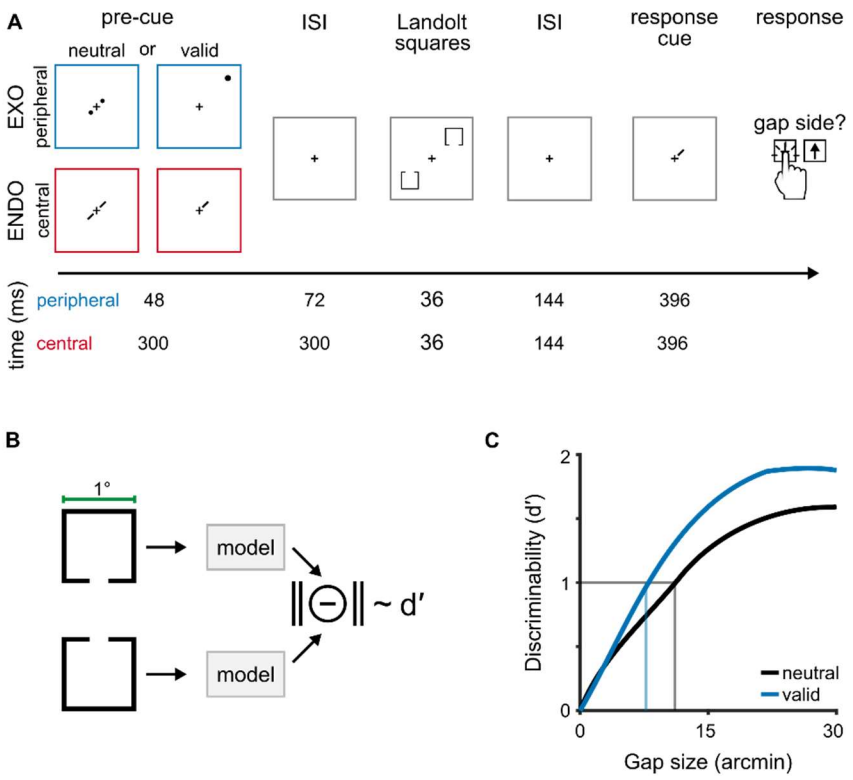

Figure S6. Behavioral protocol and modeling strategy for an acuity task.
(**A**) Behavioral protocol adapted from (11). Observers performed a standard Landolt acuity task. The gap size in each 1°-wide Landolt square varied on a trial-by-trial basis and gap thresholds were measured in conditions where attention was distributed across both target locations (neutral) or focused at a single location (valid). Peripheral cues manipulated exogenous attention (EXO) whereas central, symbolic cues manipulated endogenous attention (ENDO). On each trial, two Landolt squares appeared on one of the two main diagonals of the visual field at 9.375°. Observers judged whether a gap appeared at the top or bottom of the Landolt square indicated by a response cue displayed at the end of the trial. The response cue equated uncertainty of the target's location between neutral and valid cueing conditions. The timing information for peripheral (blue) and central (red) cueing conditions is given below each trial segment. (**B**) We modeled localization performance in this task by computing the discriminability (d′) between images of two Landolt squares. (**C**) We systematically varied gap size to simulate psychometric functions in each cueing condition. For the neutral condition, attentional gain was not included in the model. For the valid condition, we modeled exogenous attention with the narrow SF profile and endogenous attention with the broad SF profile. Gap thresholds (vertical lines) were quantified as the gap size that resulted in d′=1 (horizontal line). These gap thresholds indexed visual acuity in each condition. We fit model-derived thresholds to the behavioral data shown in **Figure 9A-B**.

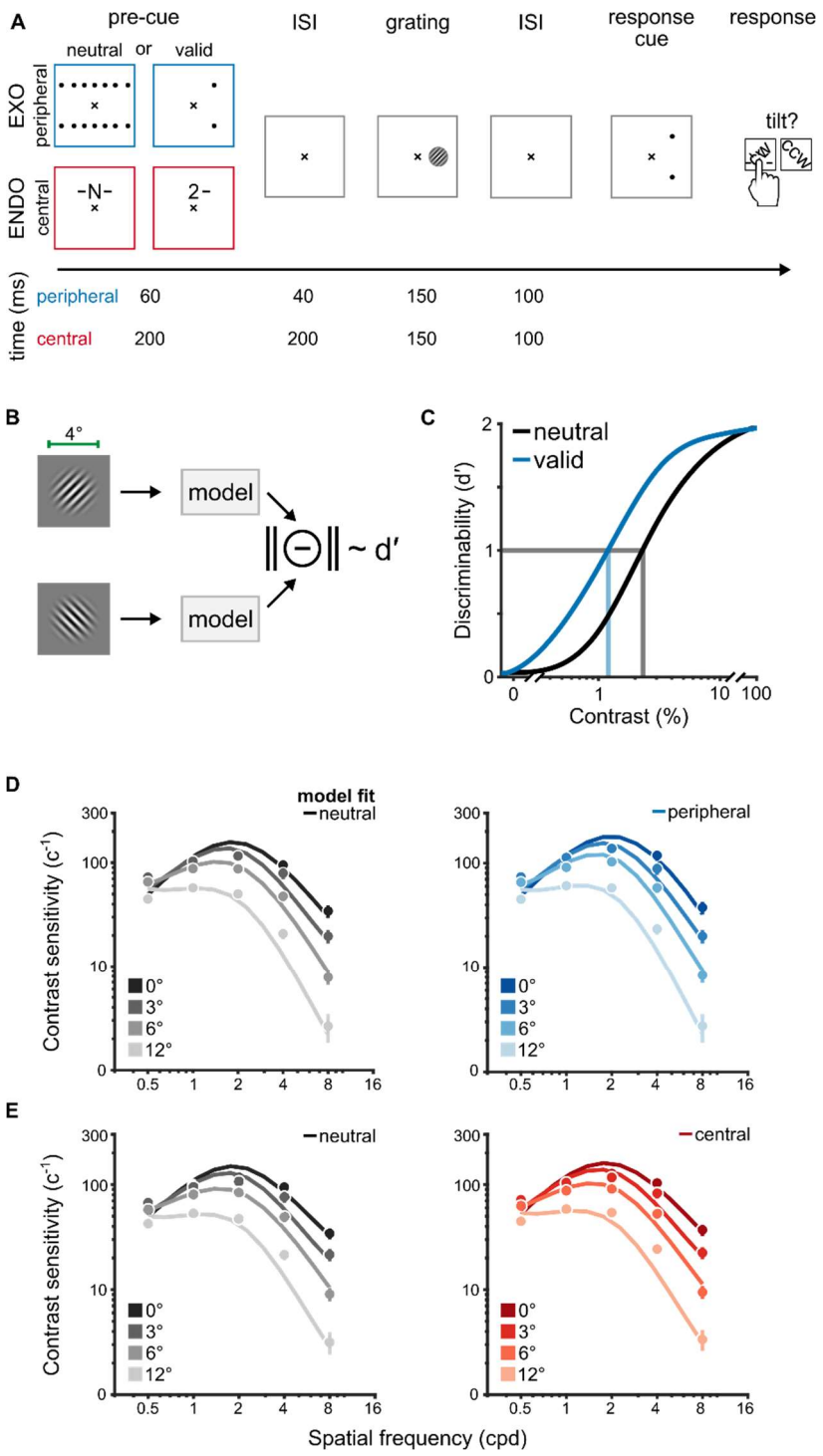
A
pre-cue
neutral or valid
ISI
grating
ISI
response cue
response
EXO
peripheral
ENDO
central
-N-
2-
tilt?
CCW
CW
time (ms)
peripheral 60 40 150 100
central 200 200 150 100
B
4°
model
model
~ d′
C
neutral
valid
Discriminability (d′)
Contrast (%)
D
model fit
neutral
peripheral
Contrast sensitivity (c⁻¹)
0°
3°
6°
12°
E
neutral
central
Spatial frequency (cpd)

Figure S7. Behavioral protocol and modeling strategy for a contrast sensitivity task. (**A**) Behavioral protocol adapted from (10). Observers performed an orientation discrimination task on 4°-wide grating stimuli that varied in their contrast, SF and eccentricity. Grating contrast varied on a trial-by-trial basis. Contrast thresholds were measured in conditions where attention was distributed across all possible target locations (neutral) or focused at a single location (valid). Peripheral cues manipulated exogenous attention (EXO) whereas central cues manipulated endogenous attention (ENDO). On each trial, a single grating appeared along the horizontal meridian at 0°, 3°, 6° and 12° of visual angle. The grating was tilted ±45° from vertical. After the onset of a response cue, observers judged whether the grating was oriented clockwise (CW) or counter-clockwise (CCW) from vertical. The response cue equated uncertainty of the target's location between neutral and valid cueing conditions. The timing information for peripheral (blue) and central (red) cueing conditions is given below each trial segment. (**B**) We modeled orientation discrimination performance by computing the discriminability (d′) between grating images of two gratings, each tilted ±45° from vertical. (**C**) We simulated contrast response functions for each combination of cueing condition, SF and eccentricity. To simulate the neutral condition, attentional gain was not included in the model. Discriminability in the valid condition was modeled with the narrow SF profile for exogenous attention (i.e., peripheral cueing condition) and the broad SF profile for endogenous attention (i.e., central cueing condition). Contrast thresholds (vertical lines) were quantified as the level of contrast that resulted in d′=1 (horizontal line). The inverse of contrast thresholds indexed contrast sensitivity and were fit to the behavioral data. (**D**) Contrast sensitivity functions for neutral (left) and peripheral cueing conditions (right). The dots and error bars depict group-average contrast sensitivity and 68% confidence intervals for each eccentricity tested in (10). The solid lines are model fits to the behavioral data. (**E**) Contrast sensitivity functions for neutral (left) and central cueing conditions (right). Visualization conventions follow those in *D*. The peak SF of the neutral contrast sensitivity functions index observers' baseline tuning preferences and are depicted as black lines in **Figure 9C-D**. The ratio between valid and neutral contrast sensitivity indexed attentional effects across SF, shown in **Figure 9C-D**.

Table S1. Model parameters. Bolded entries indicate model components.

Parameter	Description
Stimulus drive	
t_T	peak SF ($\log_2$-cpd)
t_{min}	minimum preferred SF (cpd); *fixed at 0.5*
m_T	SF tuning change across eccentricity (octaves/°)
b_T	SF FWHM bandwidth (octaves)
Contrast gain	
g_σ	gain at fovea
m_σ	slope along eccentricity
Normalization pool	
δ_f	SF pool bandwidth (octaves); *fixed at 1*
δ_θ	Orientation pool bandwidth (°); *fixed at 180*
δ_{pos}	Spatial pool width (°); *fixed at* $\frac{2}{f}$
Spatial summation	
δ_{pos}	Summation pool width (°); *fixed at* $\frac{2}{f}$
Attentional gain profile	
a_N or a_B	attentional SF tuning at the fovea ($\log_2$-cpd)
m_N or m_B	slope of SF tuning across eccentricity (octaves/°)
γ_N or γ_B	amplitude
b_N or b_B	SF FWHM bandwidth (octaves)
b_{pos}	spatial spread (°); *fixed at FWHM of 4*

Table S2. Free parameters for the fits to the neutral condition of all ten texture segmentation experiments. The mapping between the experiment labels (a-j) and the respective references is given below the table and are consistent across all tables. Bold values indicate the median and values within square brackets denote the 95% CI of the bootstrapped distribution of fitted parameters. min. = minimum; SF = spatial frequency; bw = bandwidth.

		Contrast gain		**Stimulus drive**		
parameter		g_σ	m_σ	t_T	m_T	b_T
description		*min.*	*slope*	*SF peak*	*SF slope*	*SF bw*
Experiment	a	**2.3** [2.2 2.5]	**-0.09** [-0.09 -0.08]	**1.9** [1.5 2.4]	**-0.8** [-0.9 -0.6]	**1.7** [1.6 2.0]
	b	**2.3** [2.1 2.5]				
	c	**2.7** [2.5 2.8]				
	d	**2.7** [2.6 2.8]				
	e	**2.2** [2.0 2.5]				
	f	**2.7** [2.4 2.8]				
	g	**1.9** [1.5 2.3]		**2.8** [2.4 3.1]		
	h	**1.8** [1.7 2.0]				
	i	**2.6** [2.5 2.8]				
	j	**2.7** [2.6 2.8]				

[a] Yeshurun & Carrasco, 1998 (8). *Fine-scale texture; experiment 1.*
[b] Yeshurun & Carrasco, 1998 (8). *Coarse-scale texture; experiment 2.*
[c] Talgar & Carrasco, 2002 (14). *Target meridian: lower vertical*.
[d] Carrasco, Loula & Ho, 2006 (7). *Orientation discrimination: baseline adaptation*.
[e] Yeshurun & Carrasco, 2008 (15). *Attentional cue size: cue size 1.*
[f] Yeshurun, Montagna & Carrasco, 2008 (9). *Target meridian: horizontal; experiment 2*.
[g] Yeshurun, Montagna & Carrasco, 2008 (9). *Target meridian: horizontal; experiment 1*
[h] Yeshurun, Montagna & Carrasco, 2008 (9). *Fine-scale texture; experiment 3.*
[i] Yeshurun, Montagna & Carrasco, 2008 (9). *Coarse-scale texture; experiment 4.*
[j] Barbot & Carrasco, 2017 (16). *Target meridian: intercardinal; baseline adaptation*.

Table S3. Free parameters for the fits to neutral and peripheral cueing conditions of the six exogenous attention experiments. Bold values indicate the median and values in square brackets depict the 95% CI of the bootstrapped distribution of fitted parameters. min. = minimum; bw = bandwidth; amp. = amplitude.

		Contrast gain		**Stimulus drive**			**Narrow gain profile**			
parameter		g_σ	m_σ	t_T	m_T	b_T	a_N	m_N	b_N	γ_N
description		*min.*	*slope*	*SF peak*	*SF slope*	*SF bw*	*SF peak*	*SF slope*	*SF bw*	*amp.*
Experiment	a	**1.9** [1.7 2.2]	**-0.05** [-0.07 -0.04]	**2.1** [1.8 2.8]	**-0.7** [-0.9 -0.5]	**1.6** [1.4 2.1]	**2.3** [1.8 3.0]	**-0.2** [-0.3 -0.01]	**2.9** [1.5 4.8]	**4.3** [3.0 7.8]
	b	**1.7** [1.5 2.1]								
	c	**2.6** [2.2 2.8]								
	d	**2.1** [2.8 2.5]								
	e	**1.5** [1.5 2.0]								
	f	**2.0** [1.7 2.7]								

Table S4. Free parameters for the fits to the neutral and central cueing conditions of the four endogenous attention experiments. Bold values indicate the median and values within square brackets depict the 95% CI of the bootstrapped distribution of fitted parameters. min. = minimum; bw = bandwidth; amp. = amplitude.

		Contrast gain		**Stimulus drive**			**Broad gain profile**			
parameter		g_σ	m_σ	t_T	m_T	b_T	a_B	m_B	b_B	γ_B
description		*min.*	*slope*	*SF peak*	*SF slope*	*SF bw*	*SF peak*	*SF slope*	*SF bw*	*amp.*
Experiment	g	**1.6** [1.5 2.1]	**-0.09** [-0.1 -0.06]	**3.4** [2.8 4.0]	**-0.8** [-1.0 -0.5]	**1.3** [1.1 1.6]	**1.7** [0.5 2.3]	**-0.2** [-0.3 -0.1]	**4.5** [2.1 6.6]	**3.1** [2.2 6.2]
	h	**1.7** [1.5 1.9]								
	i	**2.5** [2.2 2.8]								
	j	**1.7** [1.5 1.9]								

Table S5. Stimulus parameters for each texture segmentation experiment.

Experiment	**Line spacing** horz × vert	**Line size** width × height	**Target size** width × height	**Target meridian**	**Backward mask**
a	0.68° × 0.71°	0.1° × 0.4°	1.97° × 2.03°	horizontal	yes
b	1.36° × 1.42°	0.2° × 0.8°	3.78° × 3.84°	horizontal	yes
c	0.71° × 0.68°	0.1° × 0.4°	2.03° × 1.97°	vertical	yes
d	1.43° × 1.37°	0.2° × 1°	4.09° × 3.97°	horizontal	yes
e	0.68° × 0.71°	0.1° ×0.7°	2.28° × 2.34°	horizontal	yes
f	0.68° × 0.71°	0.1° × 0.7°	2.28° × 2.34°	horizontal	yes
g	0.68° × 0.71°	0.1° × 0.7°	2.28° × 2.34°	horizontal	yes
h	0.46° × 0.46°	0.1° × 0.2°	1.34° × 1.34°	intercardinal	no
i	0.91° × 0.91°	0.2° × 0.4°	2.47° × 2.47°	intercardinal	no
j	0.4° × 0.4°	0.1° × 0.24°	1.03° × 1.84°	intercardinal	no

Table S6. Best-fitting parameters for acuity and contrast sensitivity tasks. min. = minimum; bw = bandwidth; amp. = amplitude; acuity = acuity experiment (11); CS = contrast sensitivity experiment (10). The 95% confidence intervals show parameter values for fits to texture segmentation experiments, split by attention type.

		Contrast gain		**Stimulus drive**			**Attentional gain**				
parameter		g_σ	m_σ	t_T	m_T	b_T	a	m	b	γ	b_{pos}
description		*min.*	*slope*	*SF peak*	*SF slope*	*SF bw*	*SF peak*	*SF slope*	*SF bw*	*amp.*	*spread*
EXO	*95% CI*	[1.5 2.8]	[-0.07 -0.05]	[1.8 2.8]	[-0.9 -0.5]	[1.4 2.1]	[1.8 3.0]	[-0.3 -0.01]	[1.5 4.8]	[3.0 7.8]	-
	Acuity	2	-0.07	1.8	-0.8	1.4	2.8	-0.03	1.5	8	0.6
	CS	2.5	-0.03	1.1	-0.2	1.4	1.5	-0.01	2.3	1.5	5.2
ENDO	*95% CI*	[1.5 2.8]	[-0.1 -0.06]	[2.8 4.0]	[-1.0 -0.5]	[1.1 1.6]	[0.5 2.3]	[-0.3 -0.1]	[2.1 6.6]	[2.2 6.2]	-
	Acuity	1.5	-0.09	3	-0.9	1.1	2	-0.3	5.3	15.0	0.6
	CS	2.5	-0.04	1.1	-0.2	1.5	2.6	-0.2	4.2	1.2	5.2